

Enlargement and unaltered number of the early endosomes in  
Alzheimer's disease



CANDIDATE: Rafael DIAZ  
*Joint Master in Neuroscience*  
*Université Louis Pasteur*

SUPERVISOR: Prof. Charles DUYCKAERTS  
*Laboratoire de Neuropathologie Raymond Escourolle*  
*Hôpital de La Salpêtrière*  
*47 Boulevard de l'Hôpital*  
*75651 Paris Cedex 13.*

## SUMMARY

*It is mentioned in the literature that the early endosomes are enlarged in neuronal cell body in trisomy 21 and sporadic Alzheimer disease. This alteration has never been quantified and the mechanism of this enlargement (fusion or dilation of normal endosomes) was not determined.*

*We studied 5 Alzheimer disease (AD) cases and 5 controls. Blocks from the middle frontal gyrus were examined. A new and original technique to distinguish endosomes from lipofuscin was devised: we combined the Periodic acid-Schiff (PAS) method to reveal lipofuscin granules and immunohistochemistry of EEA1 to reveal early endosomes.*

*We, next, assessed, by point counting, the volume fraction occupied by the early endosome compartment and found it to be significantly enlarged in AD cases. We estimated the numerical density of endosomes per volume and found it to be unaltered in AD cases. The numerical density of normal (small) endosomes was, by contrast, much decreased. We concluded that the increase in the volume occupied by the endosomal compartment was related to a heterogeneous dilation of the endosomes and was not the consequence of endosomes fusion. The cause of the endosomal enlargement remains elusive but recent genetic evidence points to specific proteins.*

## INTRODUCTION

Alzheimer's disease (AD) is characterized by the presence of amyloid plaques and neurofibrillary tangles related to the aggregation and fibrillization of  $\beta$ -amyloid peptides and tau protein respectively. The amyloid plaques represent insoluble assemblies of proteolytic products of the Amyloid Precursor Protein (APP), known as amyloid- $\beta$  peptides and made of 39-42 amino acids (Glenner et al. 1984).<sup>13</sup> The mechanism of Alzheimer disease lesions is still unknown, but strong evidences indicate that aggregates of  $\beta$ -amyloid peptides represent an early event in the pathogenesis of this disease, a mechanism formalized under the name of the "cascade hypothesis".<sup>10</sup>

In the sporadic form of AD the formation of enlarged endosomes was supposed to be the earliest morphologic alteration detectable, appearing long before senile plaques formation.<sup>6</sup> The APP gene is situated on the 21 chromosome, thus the presence of three copies of APP at individuals induce a neuropathology of the AD type at an early age, around 40. The presence of three APP genes is sufficient for the development of AD. Indeed, individuals with a microduplication of the APP gene present with AD at around 52 years of age (Rovelet 2006). It is not established yet that microduplication of the APP gene is sufficient to induce the appearance of enlarged endosomes. In murine models, the APP gene is necessary but not sufficient to induce the "enlarged endosomes" phenotype (Jack Cossec, Marie-Claude Potier, in preparation).

Many disorders involve defects in the synthesis, sorting, and transport of lysosomal enzymes. Newly identified cellular regulatory pathways appear to control the targeting of proteins to lysosomes; proteolysis by lysosomal hydrolases may, in some diseases, appear to be deficient. These data suggest that the endosomal-lysosomal system may modify the functions of specific proteins. The endosomal-lysosomal system may play an important role in AD.<sup>14</sup>

By endocytosis the cells are able to internalize and to process extracellular nutrients and trophic factors; to recycle or to degrade receptors and proteins. The major route of endocytosis is mediated by clathrins, but this may also occur via caveolas, macropinocytosis or phagocytosis. The endosomal vesicles are transported to the early endosomes, the first step

of the endocytic pathway. The early endosomes are located at the periphery of the cell. They are mildly acid. Early endosomes are sorting organelles, allowing the recycling of many of the receptors back to the plasma membrane. Early endosomes cargoes reach late endosomes either by budding off transport vesicles or by directly maturing to late endosomes. The late endosomes contain internalized material from early endosomes, but also from trans-Golgi network in the biosynthetic pathway or from phagosomes in the phagocytic pathway. The late endosomes have an acidic character, mediating a final set of sorting processes prior to the delivery of the material to the lysosomes. The lysosomes are the last compartment of the endocytic pathway, being the main hydrolytic compartment of cells. As they reach a pH of 4.8, being rich in acid hydrolase, they are digesting macromolecules coming from phagocytosis, endocytosis and autophagy; they are also responsible for the turnover of cytosolic proteins and organelles (Fig. 1).

Late endosomes can be distinguished biochemically and biophysically from early endosomes and lysosomes, but debate continues over whether they represent a stable, pre-existing compartment (shuttle-vesicle model) or a transient intermediate that evolves from early endosomes (maturation model).<sup>14</sup> In the former model, a pre-existing, stable sorting endosome receives internalized substrates from early endocytic vesicles and then buds off vesicles that recycle membrane receptors to the cell surface. A second group of vesicles shuttles substrates to pre-existing lysosomes. In the alternative maturation model, the compartments are transient. Sorting endosomes accumulate endocytosed material and gradually transform into late endosomes, losing the ability to fuse with early endocytic vesicles in the process.

In tissue sections of human neocortex from normal individuals the small early endosomes are distributed close to the plasmalemma of the neurons. This localization is distinct from either the predominantly perinuclear distribution of late endosomes, the uniform cytoplasmic distribution of lysosomes, or the basal location of lipopigment granules. Normally early endosomes are spherical in shape and relatively uniform in size (100–250 nm). They are most numerous in the soma and proximal dendrites. The diameter of late endosomes and lysosomes ranges typically from 100 to 400 nm and from 50 to 400 nm respectively. Rab5<sup>3</sup> was absent from lipofuscin granules, late endosomes and lipofuscin granules which are identified on the basis of their size (0.5–1.5  $\mu\text{m}$ ) and on their autofluorescence attributed to lipopigments. They are concentrated in the basal region of the cell soma.

Cataldo and Nixon<sup>14</sup> have studied the cellular mechanisms underlying  $\beta$ -amyloidogenesis in sporadic and familial AD, Down syndrome (DS) and the roles of the endocytic pathway and lysosomal system in APP processing leading to A $\beta$  generation (Cataldo et al, 2004). They claim that abnormalities of neuronal early endosomes in pyramidal neurons of the neocortex are the earliest known disease-specific pathology of sporadic AD, appearing before significant amyloid deposits and neurofibrillary pathology develop – although this claim is difficult to prove in the context of sporadic AD. The major evidence is the coincidence between the appearance of enlarged endosomes and the initial rise in soluble A $\beta$ 40 and A $\beta$ 42 peptides, occurring before visible amyloid deposition.<sup>5,4,12</sup>

According to Cataldo and Nixon (2008), the prevalence of abnormally enlarged endosomes is ten-fold higher in AD brains than in controls. Enlarged endosomes in AD brain measure an average of 487 nm in diameter (average diameter per brain ranged from 400 to 620 nm). Enlarged endosomes profiles were found principally in at-risk pyramids of laminae III and V. In AD individuals, endosomes display up to 32-fold larger volumes than in controls. Endosomal enlargement is responsible for an average 2.5-fold increase in total endosomal volume per neuron, implying a marked increase in endocytic activity<sup>2</sup> that further induces endocytic perturbations in neurons<sup>7</sup> (Fig 2).

Altered expression and distribution of endosome functional markers occur in AD. The markers of endocytosis (Rab5), fusion (EEA1, Rabaptin5) and recycling (Rab4) are all altered likely reflecting up-regulated endocytosis. EEA1 is a downstream effector protein of vesicle membrane fusion and docking, associated with rab5 which plays a critical role in endocytosis.<sup>4,5</sup> Like Rabaptin-5, EEA1 forms homodimers. It contains two Rab5 binding sites in its N-terminal zinc finger and could play a role in endosome docking.<sup>2,17</sup>

Enhanced endocytic activity could be responsible for an increased interaction between APP and BACE, the protease that cleaves its N-terminus, enhancing A $\beta$  production. This increased endocytic activity could be the essential pathogenetic mechanism in sporadic AD and DS. It should be stressed that mutation of the PS1 and PS2 gene is not associated with enlarged endosomes, indicating that altered endocytosis is not a consequence of A $\beta$  deposition.<sup>4</sup>

The results of Cataldo et al.<sup>3,6</sup> showing the presence of enlarged endosomes are based on a method of limited specificity, not allowing a fine distinction between the enlarged endosomes and the lipofuscin grains. Moreover the mechanism and effect of endosomes enlargement have not been quantitatively assessed: does it result from fusion of the endosomes (in that case the number of endosome would decrease)? Is it the consequence of pure enlargement of a population of endosomes (in that case the number of endosomes would remain similar)? Does it induce an increase in the volume fraction occupied by the endosomal system? The aim of the study was to develop a sensitive technique of immunohistochemistry for the identification of enlarged endosomes with high specificity on brain sections and to determine the quantitative parameters of endosome enlargement: number of normal and of enlarged endosomes, volume fraction occupied by the endosomes (Fig 3).

## MATERIAL AND METHODS

### Tissue

Postmortem brain tissues were examined at Raymond Escourolle Neuropathology Laboratory. After fixation of the brains in a buffered solution of 4 % formaldehyde and macroscopic examination, samples from hippocampus and isocortex were embedded in paraffin, cut at 5  $\mu$ m of thickness and examined after haematein & eosin staining, and immunolabelling by Tau (clone AT8, Thermo Fisher Scientific) and A $\beta$  (clone 6F/3D, DakoCytomation) antibodies. The cases were staged according to Braak and Braak.<sup>1</sup>

The patients group consisted in 5 cases meeting the criteria for severe stage AD (numerous plaques and tangles in the transentorhinal, entorhinal/hippocampal cortices and in the neocortex; Braak stage V–VI). The control groups consisted in 5 age-matched cases, age ranging from 62 to 80, which were found to be neuropathologically normal (isocortex, entorhinal cortex/hippocampus devoid of plaques and neurofibrillary tangles). The medial frontal gyrus (Brodmann area 10) was chosen since it allowed the best contrast between cases with and cases without lesions. The hippocampus, which is involved at a very early stage of the disease, is almost invariably altered in old patients. The first experiments were performed on paraffin-embedded sections, but the results were unsatisfactory: the endosomes, immunolabelled by EEA1 antibodies, could barely be identified. The early endosomes were therefore evaluated in vibratome sections of formalin-fixed tissue blocks. Ten-micrometer-thick postmortem brain tissues from the frontal cortex of subjects have been studied.

### Immunohistochemical:histochemical (IHC:HC) stains

Early endosomes were shown by immunohistochemistry using a commercial polyclonal antibody (rabbit) directed against early endosome antigen 1 EEA1 (Affinity Bioreagents, Saint Quentin en Yvelines).

The first attempts on paraffin sections indicated that it was often difficult to distinguish the brown color of the lipofuscin pigments and oxidized DAB. We first tried unsuccessfully to

mask lipofuscin granules by various pre-treatments (Sudan black, potassium permanganate).<sup>15</sup> Following a previous report, we then turned to an alternative method consisting in revealing lipofuscin in a color different from the color of oxidized DAB<sup>8</sup>. Ziehl method with fuchsin showed the lipofuscin pigments in red, but the stain did not resist the dehydration and, moreover, the color was so intense that it masked the immunolabelling. The staining with Nile Blue sulphate<sup>9</sup> was also too bright and dehydration bleaches the section as well. Finally, the Periodic Acid Schiff (PAS) technique stains very distinctly the lipofuscin granules in a bright purple, easy to distinguish from the brown color of DAB. PAS resisted dehydration and did not hamper subsequent immunohistochemistry. Several trials indicated, however, that PAS technique should rather be realized after the immunohistochemical staining.

### **Paraffin or vibratome sections?**

Paraffin sections, which we first used, may be thin (5 µm) and exhibit an unmatched optical quality. However, to reach it, the sections have to go through a dehydration cycle, starting from alcohol 70 % to 80%; 90% and finally 100 %, followed by several batches of xylene. This process, taking the lipids away, makes the section more transparent and the labeling of proteins more delicate. The lipids of the membrane are solubilized and the identity of small membranous organelles may be lost. The immunolabelling with EEA1 in paraffin sections was blurred. We considered that this could have been due to the alcohol and xylene treatment. This is why we used vibratome sections, obtained by submitting a formaldehyde fixed block of tissue to a vibrating razor blade. This technique produces slides in which the membranes are preserved. We found out that good EEA1 immunohistochemistry could be obtained with these sections. The final protocol combined EEA1 immunohistochemistry to identify the endosomes and PAS (to show the lipofuscin granules).

### **IHC:HC protocol (Fig 4)**

- Formalin-fixed cortical samples were cut with a vibratome at a nominal thickness of 10 µm. Sections were incubated in 2 ml of tris-buffered saline TBS (50 mM Tris, 150 mM sodium chloride, drops of HCl, pH 7.4) in a multiwell tissue culture plate. The sections were stored in TBS overnight at 4°C.
- A 1:100 dilution of a 30% hydrogen peroxide stock solution in methanol was prepared just before use to inactivate endogenous peroxidase activity in the tissue. Sections

were left in the solution and the plate was gently shaken on a rocking platform for 30 min. Sections shrank and wrinkled in methanol.

- After discarding methanol hydrogen peroxide the sections were rinsed briefly in TBS, and washed in 2 ml of TBS for 10 min, under gentle shaking, in order to remove all traces of methanol. This rehydration causes the re-expansion of the sections (wrinkles gradually disappeared).
- The vibratome sections were transferred to 250 ml Pyrex glass, each containing 200 ml of citrate buffer (50 mM trisodium citrate dihydrate, pH 6.0). The isotonic 150 mM sodium ion concentration of this buffer prevented shrinkage or expansion of the sections during heating. The total irradiation time (for 250 ml) in the microwave was 7 min. Irradiation was performed at full power until the buffer just began to boil (2 minutes). The setting was further changed to autodefrost mode (intermittent microwaves at 200–300 W, cycling on for 5–10 s every 30 seconds) and the sections were irradiated for 5 more minutes. During this period, the solution remained at a temperature of approximately 95° and did not boil. The Pyrex glass was removed from the microwave. The solution was allowed to cool around 30 minutes until the temperature decreases below 40°C. Using a small and soft paint brush, the sections were transferred to a multiwell plate containing TBS, and carefully unfolded to remove folds and wrinkles. The sections were further washed twice for 5 minutes in 2 ml of TBS on a rocking platform.
- The sections were washed three times in 2 ml of diluting buffer DB (TBS, pH 7.4, 1% normal goat serum, 2% bovine serum albumin, 0.4% Triton X-100) for 10 min on a rocking platform. As the sections absorbed protein in the presence of non-ionic detergent, wrinkles observed with solutions containing triton X-100 disappeared.
- The DB was removed, and 2 ml of sterile-filtered 20% serum (normal goat serum in TBS) was added for 1 h to block non-specific protein binding sites in the tissue sections.
- All antibody stock solutions were centrifuged at 15 000 rpm in microfuge tubes for 5 min just before preparing working dilutions. This removed partially denatured antibody aggregates that non-specifically bind to the tissue sections, increasing the background staining. Afterwards the sections were incubated with polyclonal EEA-1 antibody, dilution 1/250 in DB, overnight at 4°C. With 1/125 dilutions the background staining was stronger. 1/500 and 1/000 dilutions of the antibody gave negative results.

- The sections were washed three times for 10 min in 1 ml of DB and incubated in Biotinylated secondary antibodies (bottle A of KIT Dako REAL) for 1 h.
- The sections were washed three times for 10 min in 1 ml of DB and incubated in Streptavidin Peroxidase HRP (bottle B of KIT Dako REAL) for 1 h.
- The sections were washed three times for 10 min in 1 ml of TBS and incubated in DAB + Chromogen (bottle C+D of KIT Dako REAL), dilution 1/200 in HRP substrate buffer for 3 minutes. Sections turned light to dark brown depending on the amount of non-specific background immunoreactivity. The staining was controlled by direct microscopical observation. Two to 3 min of staining was usually optimal. The reaction was over after two subsequent transfers of each section, using a small paint brush, in a second culture plate containing 2 ml of deionized water per well.
- The water was removed with a micropipette and the sections were washed twice for 10 min in 2 ml TBS.
- Some practice is required for this step, especially if one intends to mount several sections per slide. Using a small soft bristle paint brush and a Petri dish filled with TBS, the sections were picked up on a Super Frost® (silanized) glass slides. The excess liquid was removed. The sections were left to dry, face up on a flat surface, overnight at room temperature to firmly affix them to the slides.
- On the next day, the slides were incubated in 1% periodic acid solution for 5 minutes and then washed in distilled water for 5 minutes.
- The slides were further incubated in Schiff reagent (Merck) for 15 minutes and washed in tap water for 10 minutes.
- Counterstaining was performed in Mayer's hemalun for 5 seconds followed by washing in tap water for 5 minutes.
- The slides were dehydrated in three ascending alcohol solutions, 15 minutes in each alcohol, and cleared with xylene for 30 minutes.
- DPX mounting media was used to coverslip.

## Stereology

The quantitative evaluation of the density of early endosomes raised several problems: 1) endosomes are small objects at the limit of the resolution power of light microscopy 2) they are so abundant in the cytoplasm that it is impossible to count them all 3) their size changes: since the probability of including enlarged endosomes in the section is higher than the probability for small endosomes, a naïve counting would bias the results toward an overestimation of the large endosomes.

To deal with these problems, we decided to use two methods of assessment:

1) The measurement of the area occupied by the endosome in relation with the total area of the cytoplasm. This "area density" is directly proportional to the "volume density" according to Delesse principle ( $V_v = A_A$ )<sup>18</sup>. The point counting method was used. For this, a rectangle lattice with 368 test points ( $P_T$ ), and a distance ( $d$ ) between the test points of 2.85  $\mu\text{m}$  was drawn and attached to the video screen. The picture of a microscopical field was examined on the screen through a camera adapted to the phototube of a microscope. The numbers of test points located on EEA1 immunoreactive structures ( $N_+$ ) and of test points located outside them ( $N_-$ ) were evaluated. The areal fraction  $A_A$  was estimated by the ration  $N_+ / (N_- + N_+)$ . Ten fields were evaluated per case. A pilot study showed that with this sampling scheme, the coefficient error was sufficient low – between 3 and 5.3 %.

2) The evaluation of the number of endosomes. We used very small samples of 8,12  $\mu\text{m}^2$  (to decrease the number of object) and the disector method<sup>16</sup> in order to avoid overestimation of large endosomes. The thickness of the microscopical section was determined with a microcator and was found to be 5,8  $\mu\text{m}$  on average. The volume of the sample was thus 8.12 x 5.8 = 47.1  $\mu\text{m}^3$ . This volume was systematically examined from the upper surface of the slide to the lower surface using an objective with a high numerical aperture (NA 1.25; objective x100). The micrometric screw was moved to examine successively the various optical planes. Only the objects which were seen and disappeared with the change of focus were counted. This so-called optical microdisector results in counting only the inferior pole of the objects (here the endosomes). The pole is a virtual point of dimension 0 that is, therefore, not biased. Five samples were counted per case.

## RESULTS

### Qualitative observation with the combined IHC:HC staining protocol

On post mortem material, it is difficult to distinguish lipofuscin granules from an immunohistochemical or immunofluorescent signal. Lipofuscin, indeed, appears brown when DAB has been used as chromogen; it is autofluorescent, and may therefore be mistaken for the red or green fluorescence of the secondary antibody. The extinction of fluorescence by Sudan black appeared to be difficult to control and it could additionally extinct the immunofluorescence. Therefore a method that would allow distinction of the positive and the spurious signals by the means of different colors was needed.

The combined IHC:HC (Fig 5) allowed a fine differentiation of lipofuscin from enlarged endosomes and a colocalization of these two endocytic pathway elements in the same tissue section. With vibratome we obtained a good staining of the endosomes in brown and a strong staining of lipofuscin in red when the PAS incubation time was 30'. We reduced the time of PAS staining by half and found that the equilibrium between the brown of the immunohistochemistry and the purple of the PAS was then satisfactory. This novel approach indicated that although there is some detectable co-localization, most granules of lipofuscin and enlarged endosomes occupy distinct cellular compartments in neurons of normal, age-matched controls, and of AD brains (Fig6).

Moreover, the lipofuscin granules were, on average, threefold larger than enlarged endosomes. As described previously in the literature<sup>3</sup>, early endosomes were spherical in shape and relatively uniform in size (100-250nm) in brains of control individuals. In AD brains, we found that the early endosomes are significantly larger, presenting with a diameter between 400 nm to 1.4  $\mu$ m (Fig7).

### **Surface density of endosomes per neuron**

The total surface occupied by early endosomes (both normal and enlarged) was 49 % +/- 2.9 % in controls (mean +/- SEM) and 66 % +/- 2 % in AD cases ( $t= 4,4$ ;  $p < 0,003$ ) (Fig 8,9).

### **Number of endosomes per $\mu\text{m}^3$**

The density of endosomes was 0,52 +/- 0,04 /  $\mu\text{m}^3$  for AD cases and 0,42 +/- 0,03 for the controls. The difference was not statistically significant ( $p=0,10$ ). Since the normal endosomes were found to be recognizable by their size and them were totally included in the volume, we also evaluated the density of normal endosomes. We found a value of 0.12 +/- 0.008 /  $\mu\text{m}^3$  for AD cases and 0.26 +/- 0.013 for controls. The difference was highly significant (t test:  $p=0.00001$ ) (Fig 10, 11).

## DISCUSSION

We have evaluated the volume fraction occupied by the early endosome compartment and discovered that it was increased in the AD patients in a statistically significant way. Using the disector unbiased method we have shown that the numerical density of the endosomes per  $\mu\text{m}^3$  was not modified, although the proportion of "normal" endosomes was found to be low in AD.

### **Lipofuscin subcellular localization**

Cataldo et al.<sup>3</sup> have shown that lipofuscin was concentrated in the basal pole of the cell soma. Contrarily to this observation, I have found the lipofuscin, often grouped as grains, were distributed throughout the cytosol. The combined IHC:HC staining protocol made for lipofuscin and enlarged endosomes in AD brains was developed to allow the differentiation between these two structures in the neuron and to eliminate possible false positive lipofuscin staining artifacts. Moreover, this new combined IHC:HC protocol can be used to investigate the spatial distribution of other proteins relative to lipofuscin.

Differential staining is important but there are other features to distinguish between lipofuscin and enlarged endosomes, the larger size of lipofuscine vesicles as compared to enlarged on non-enlarged endosomes and their different shapes: square and rectangular forms (lipofuscin granules) as opposed to circular (endosomes).

### **Modification of the endosomal compartment in AD**

We measured the surface density of endosomes and the total number of endosomes in AD and controls and found a significant difference with the surface density measurement. For the first time, we evaluated quantitatively the increased volume fraction of the early endosomal compartment. This increase is quite significant and suggests that there is an increase endocytosis in AD (although other scenarios are possible). Two main possibilities are then to be considered: the enlarged endosomes could be the consequence of the fusion of normal endosomes. In this case, one would expect a decrease in the total number of endosomes. In

another hypothesis, one could imagine that all or some of the normal endosomes becomes larger. In this hypothesis, the total number of endosomes would be unaltered. This is, indeed, what we found. The total number of endosomes per  $\mu\text{m}^3$  was not significantly different between AD and controls. The enlargement with unaltered number could take place in two different manners: all of the normal endosomes could enlarge slightly (homogeneous hypothesis) or some of them would become much enlarged (heterogeneous hypothesis). The persistence of a normal population of endosomes in the AD cases is in favor of this last hypothesis.

In conclusion, our study allows describing a scenario of the alteration of the early endosome compartment. An initial alteration that remains to be determined induces the enlargement of a significant portion of the endosomal compartment without fusion. The initial alteration may be discussed: it could be secondary to an increased endocytosis. However, the process seems to be quite specific to AD and it is therefore plausible that a specific change modifies the compartment.

This specific change could also be a defect in the clearance of the early endosome from the periphery of the cytoplasm – a mechanism in which multiple proteins are involved. A study, in preparation in the laboratory, has tried to identify the specific genes that were necessary to obtain the "enlarged endosome" phenotype in trisomy 21. Partial duplication has limited the number of possible genes. One of them seems to be specifically involved.

# ANNEXES

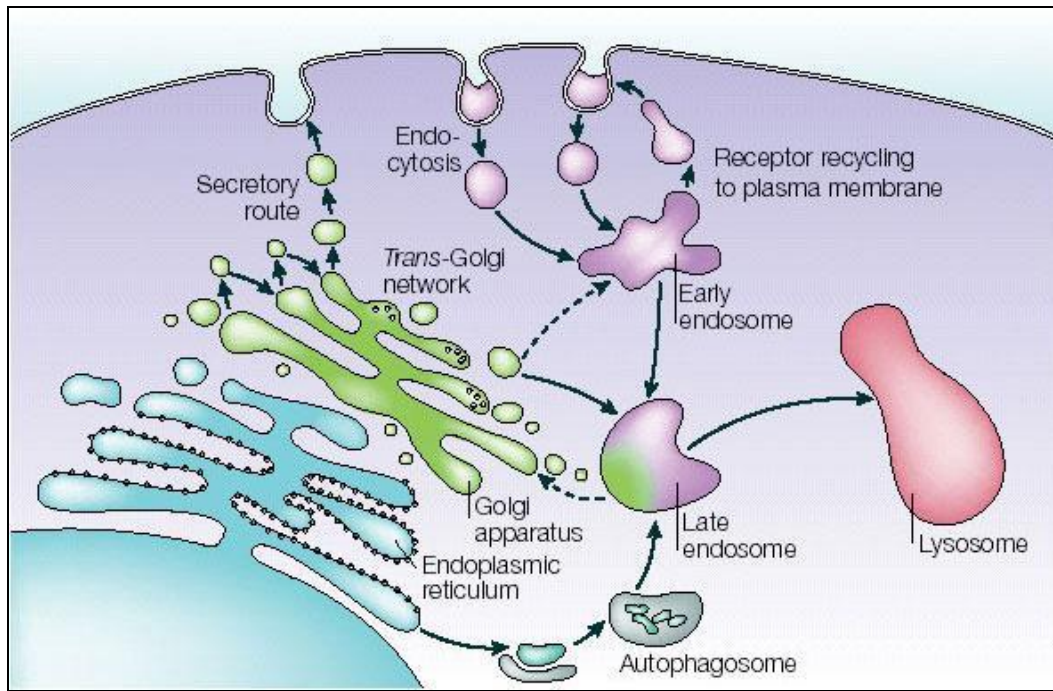


Fig 1. The endosomal/lysosomal system mediates the internalization, recycling, transport and breakdown of cellular and extracellular components and facilitates dissociation of receptors from their ligands.<sup>11</sup>

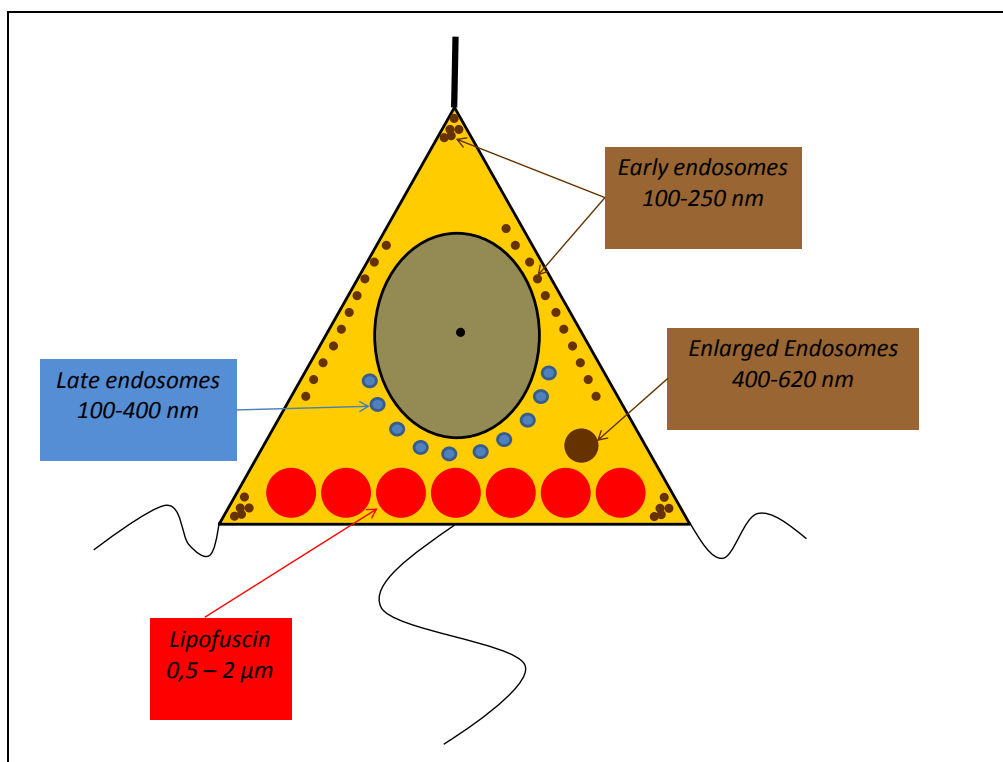
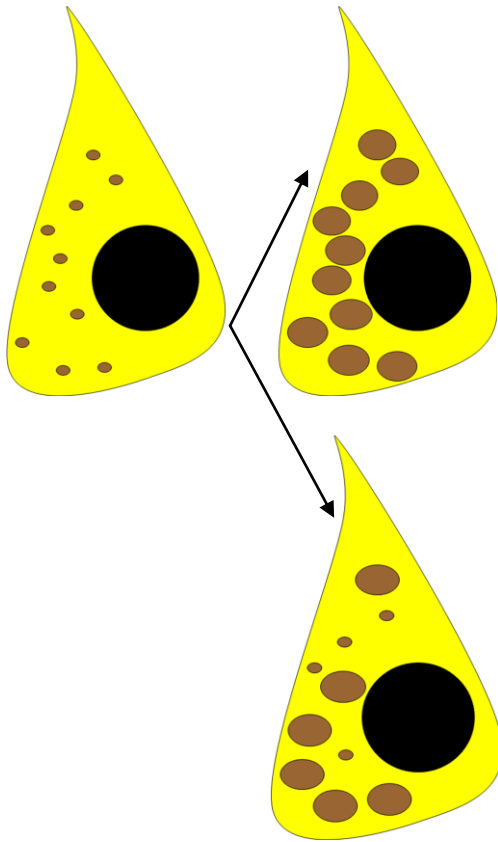


Fig 2. Distribution and sizes of the endosomal/lysosomal system in a pyramidal neuron, according to Cataldo et al.<sup>3</sup>

CONTROL

ALZHEIMER'S  
DISEASE



**Hypothesis 1A:** Enlargement of endosomes, the number of endosomes remains similar.

*Homogeneous hypothesis: all of the normal endosomes enlarged*

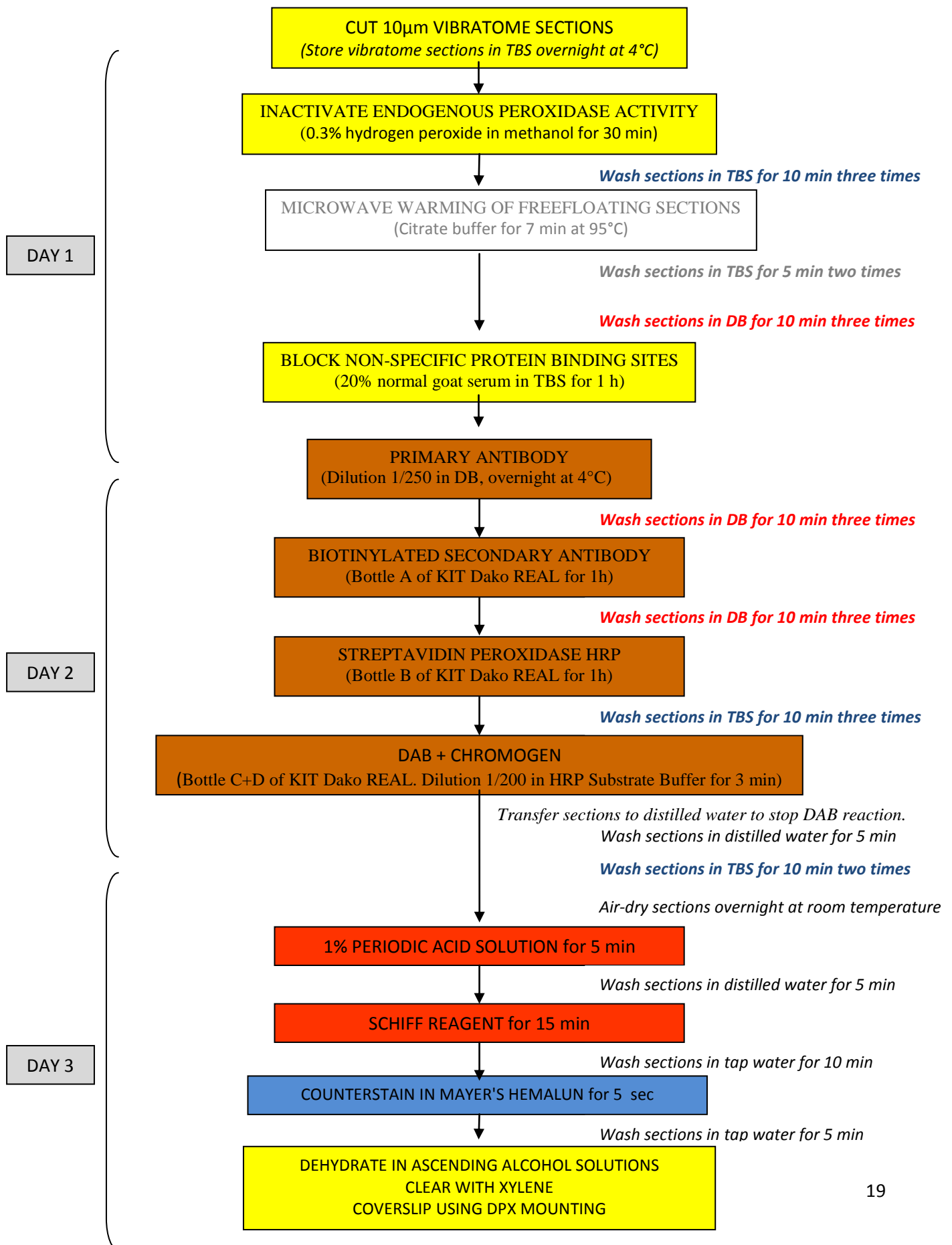
**Hypothesis 1B:** Enlargement of endosomes, the number of endosomes remains similar.

*Heterogeneous hypothesis: some of the normal endosomes become enlarged*

**Hypothesis 2:** Fusion of endosomes, the number of endosomes decreases.

Fig 3. Hypothesis of the mechanisms of endosome enlargement.

Fig 4: IHC:HC protocol



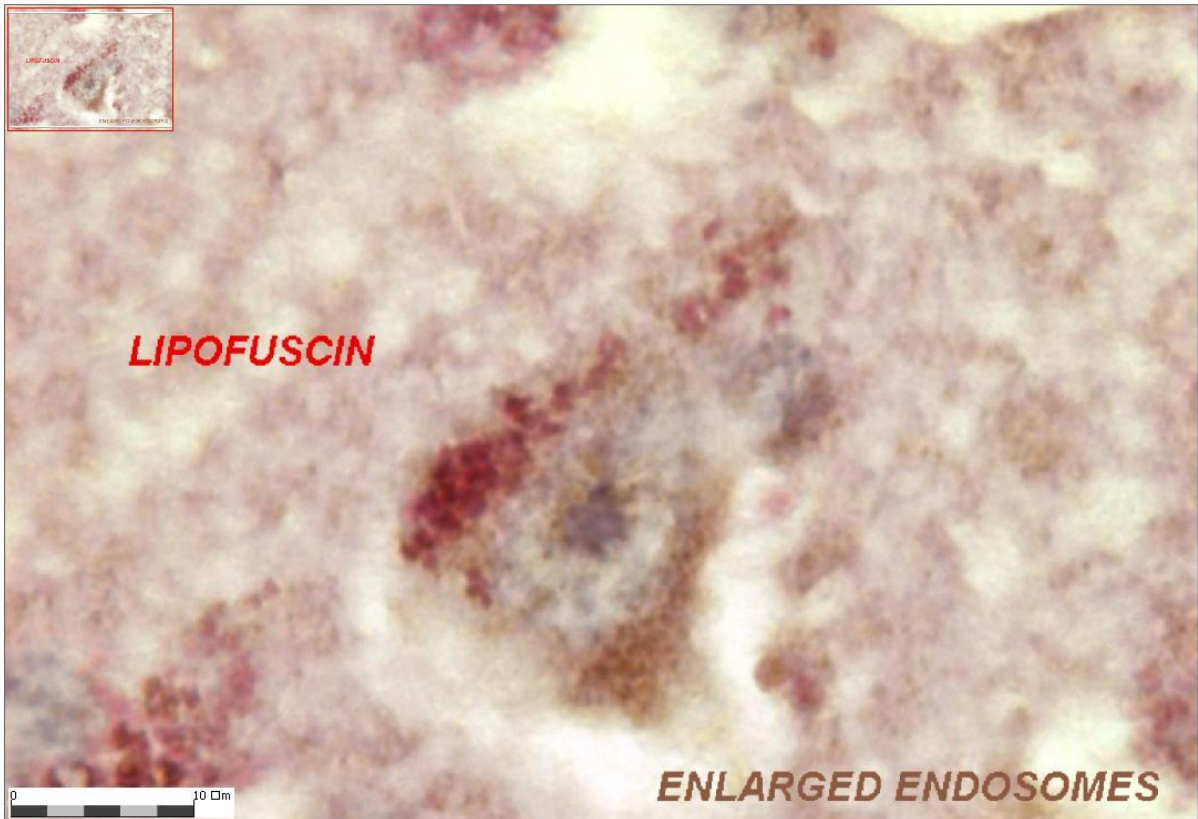


Fig 5: Combined IHC:HC staining of a pyramidal neuron of AD brain. Lipofuscin in red in the left side and enlarged endosomes in brown in the right side of the neuron.

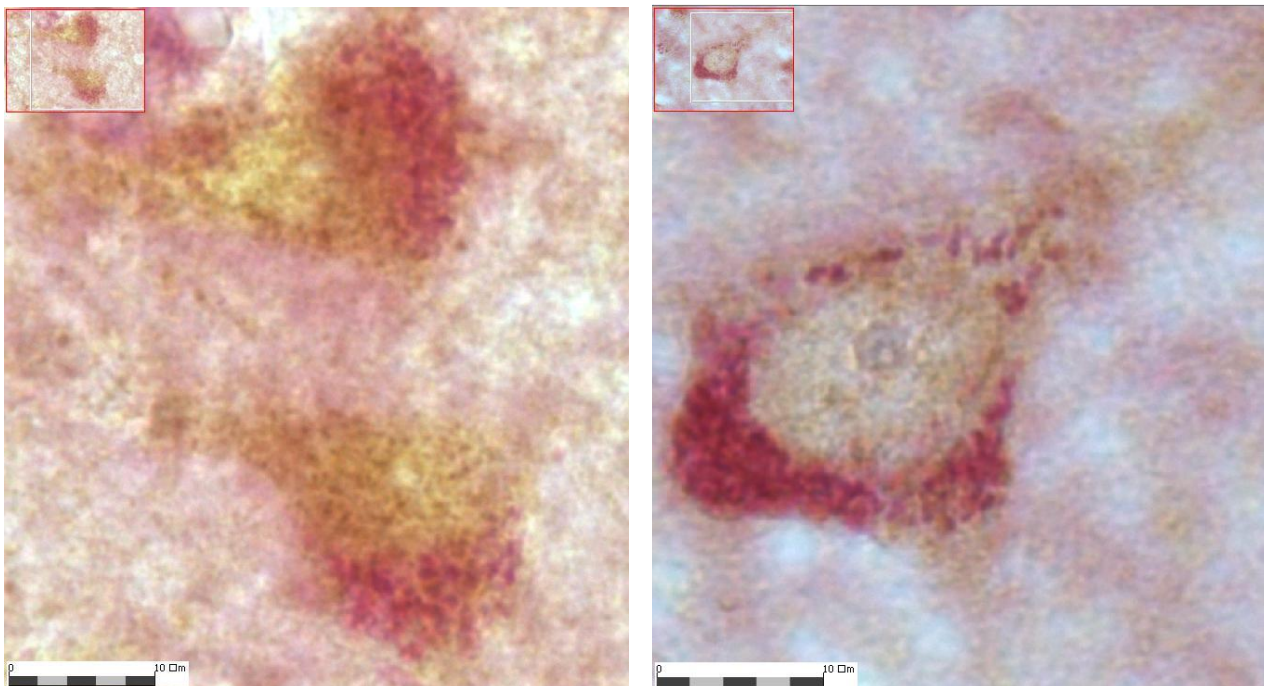


Fig 6: Combined IHC:HC staining. In the left side pyramidal neurons of AD brain with predominance of enlarged endosomes. In the right side a pyramidal neuron of control brain with predominance of normal endosomes.

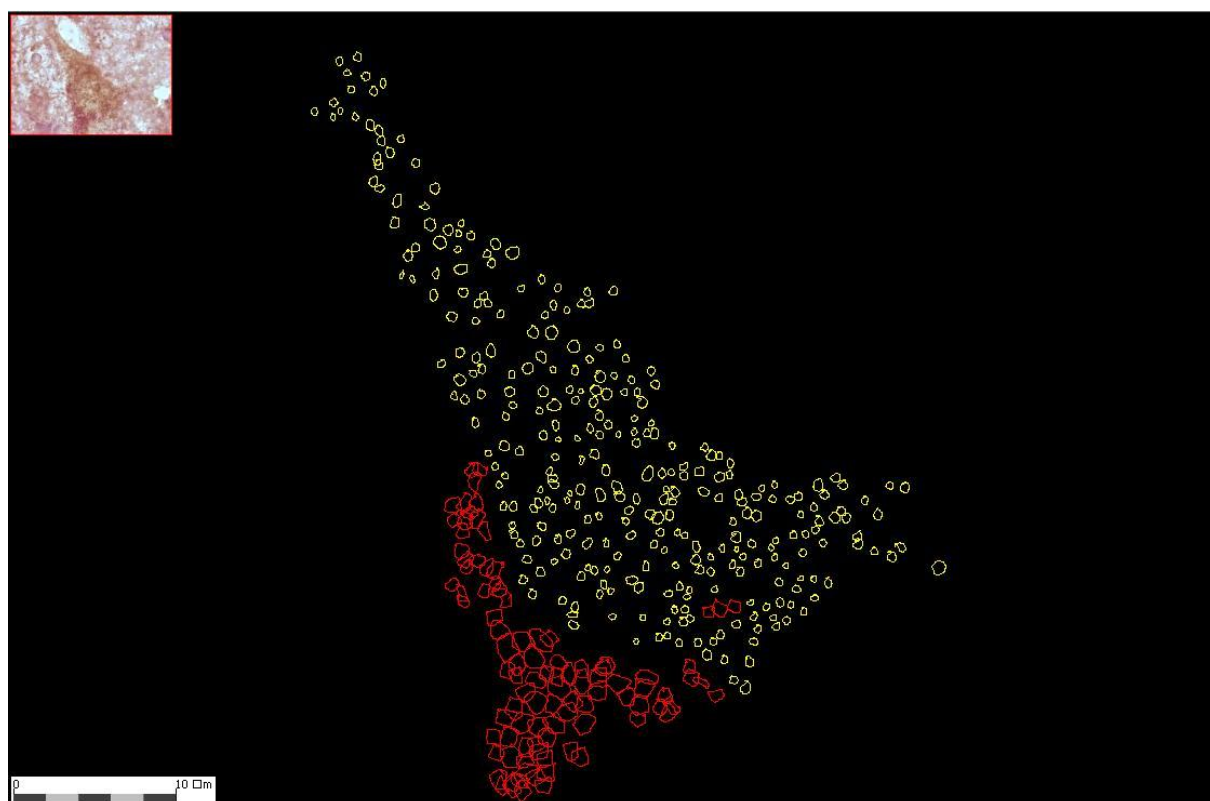
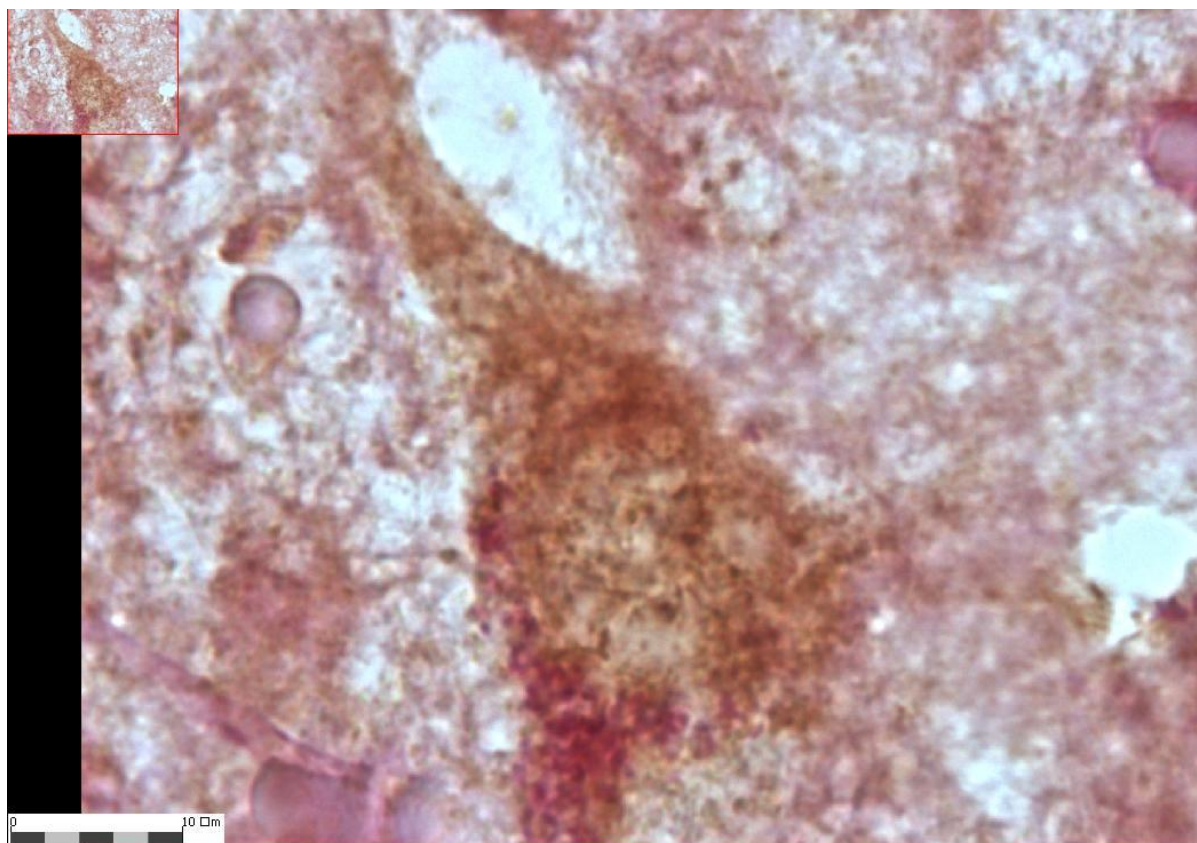


Fig 7: Distribution and size of lipofuscin and enlarged endosomes in a pyramidal neuron of AD brain.

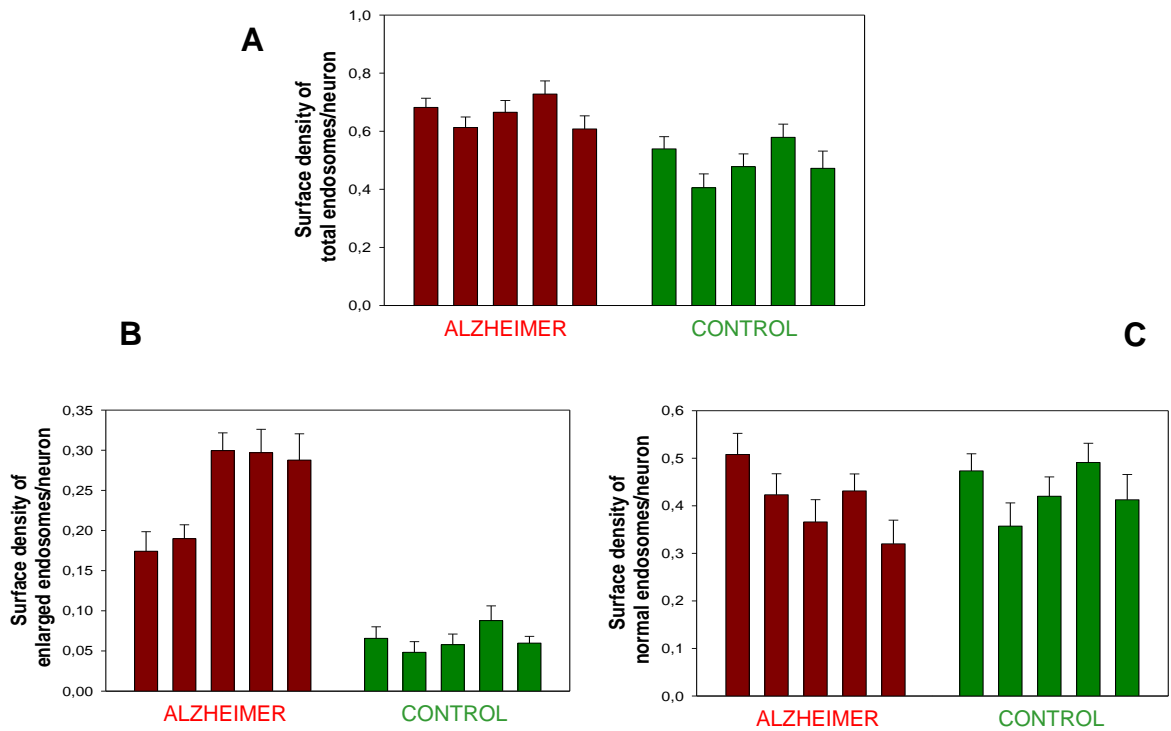


Fig 8: Surface density of endosomes per neuron. *A*, Total endosomes per neuron. *B*, Enlarged endosomes per neuron. *C*, Normal endosomes per neuron.

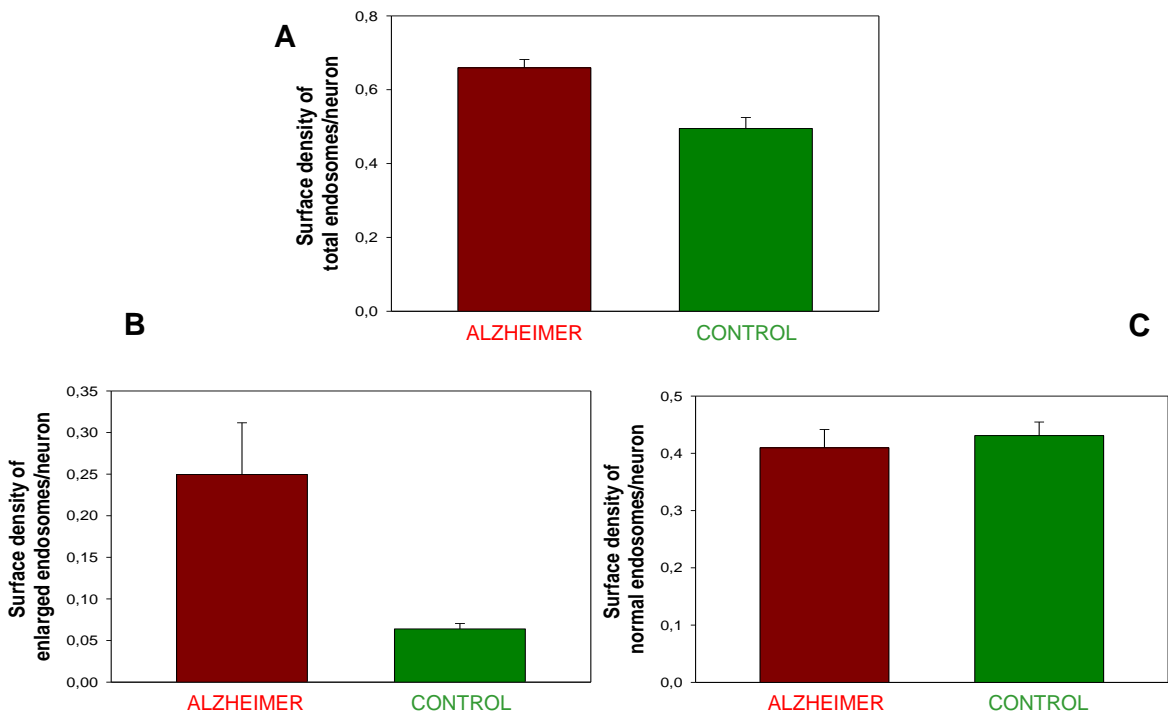


Fig 9: Mean of the surface density of endosomes per neuron. *A*, Total endosomes per neuron. *B*, Enlarged endosomes per neuron. *C*, Normal endosomes per neuron.

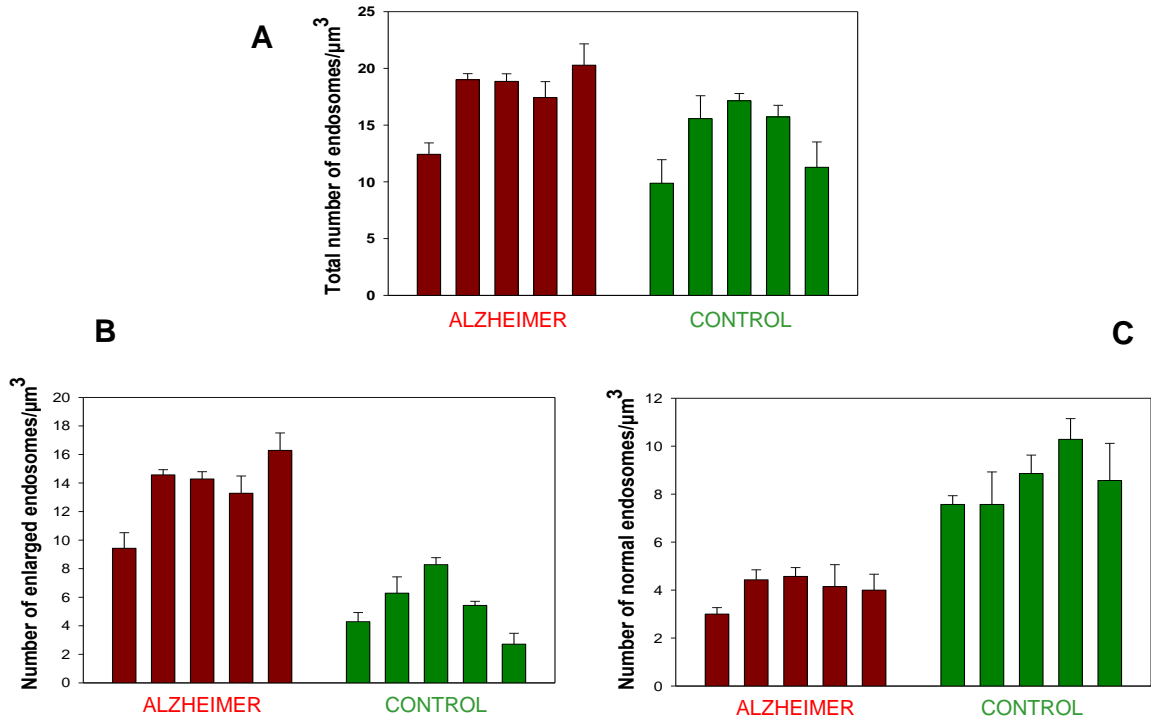


Fig 10: Number of endosomes per  $\mu\text{m}^3$ . *A*, Total endosomes per  $\mu\text{m}^3$ . *B*, Enlarged endosomes per  $\mu\text{m}^3$ . *C*, Normal endosomes per  $\mu\text{m}^3$ .

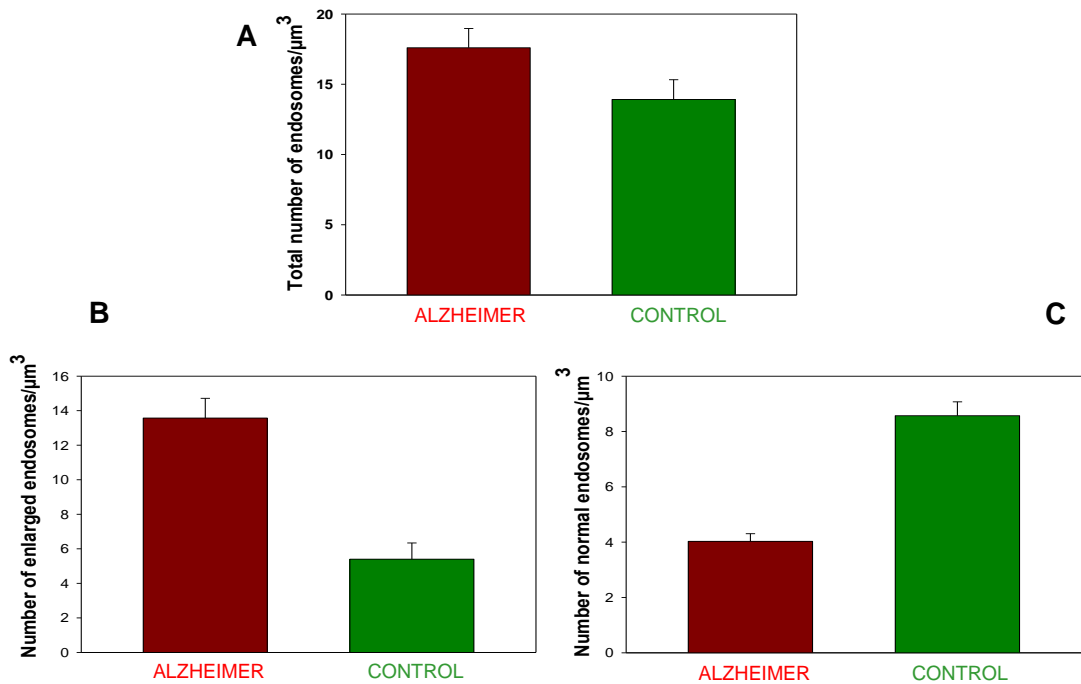


Fig 11: Number of endosomes per  $\mu\text{m}^3$ . *A*, Total endosomes per  $\mu\text{m}^3$ . *B*, Enlarged endosomes per  $\mu\text{m}^3$ . *C*, Normal endosomes per  $\mu\text{m}^3$ .

## BIBLIOGRAPHY

1. Braak H, Braak E (1991) Neuropathological staging of Alzheimer-related changes. *Acta Neuropathol.* 82(4):239-59
2. Callaghan J, Simonsen A (1999) The endosome fusion regulator early-endosomal autoantigen 1 (EEA1) is a dimer. *Biochem. J.* 338, 539-543
3. Cataldo AM, Jody LB, Pieroni C, Nixon RA (1997) *Increased neuronal endocytosis and protease delivery to early endosomes in sporadic Alzheimer's Disease: Neuropathologic evidence for a mechanism of increased  $\beta$ -amyloidogenesis.*
4. Cataldo AM, Peterhoff CM, Troncoso JC, Gomez-Isla T, Hyman BT, Nixon RA (2000) Endocytic pathway abnormalities precede amyloid  $\beta$  deposition in sporadic Alzheimer's disease and Down syndrome. *Am J Pathol* 157(1): 277–286
5. Cataldo AM, Petanceska S (2004) A $\beta$  localization in abnormal endosomes: association with earliest A $\beta$  elevations in AD and Down syndrome. *Neurobiology of Aging* 25: 1263–1272.
6. Cataldo AM, Petanceska S, Terio NB, Peterhoff CM, Durham R, Mercken M, Mehta PD, Buxbaum J, Haroutunian V, Nixon RA (2004) A $\beta$  localization in abnormal endosomes: association with earliest A $\beta$  elevations in AD and Down syndrome. *Neurobiol Aging* 25: 1263-72.
7. Cataldo AM, Mathews PM, Boiteau AB, Hassinger LC, Peterhoff CM, Jiang Y, Mullaney K, Neve RL, Gruenberg J, Nixon RA (2008) Down syndrome fibroblast model of Alzheimer-related endosome pathology: accelerated endocytosis promotes late endocytic defects. *Am J Pathol* 173(2):370-84

8. D'Andrea MR, Nagele RG, Gumula NA, Reiser PA, Polkovitch DA, Hertzog BM, Andrade-Gordon P (2002) Lipofuscin and Abeta42 exhibit distinct distribution patterns in normal and Alzheimer's disease brains. *Neurosci Lett* 323: 45-9.
9. Dunnigan MG (1968) The use of Nile blue sulphate in the histochemical identification of phospholipids. *Stain Technol* 43: 249-56
10. Hardy JA, Mann DMA, Wester P (1986) An integrative hypothesis concerning the pathogenesis and progression of Alzheimer's disease. *Neurobiol Aging* 7: 489.
11. Jeyakumar M, Dwek RA, Butters TD, Platt FM (2005) Storage solutions: treating lysosomal disorders of the brain. *Nat Rev Neurosci.* 6(9):713-25.
12. Laifenfeld D, Patzek LJ (2007) Rab5 mediates an amyloid precursor protein signaling pathway that leads to apoptosis. *J. Neurosci* 27(27):7141–7153
13. Kang J, Lemaire H-G, Unterbeck A, Salbaum JM, Masters CL, Grzeschik KH, Multhaup G, Beyreuther K, Muller-Hill B (1987) The precursor of Alzheimer's disease amyloid A4 protein resembles a cell-surface receptor. *Nature* 325: 733-736).
14. Nixon RA, Cataldo AM. (1995) The endosomal-lysosomal system of neurons: new roles. *Trends Neurosci.* 18: 489-496.
15. Schnell SA, Staines WA, Wessendorf MW (1999) Reduction of lipofuscin-like autofluorescence in fluorescently labeled tissue. *J Histochem Cytochem* 47: 719-30
16. Sterio DC (1984) The unbiased estimation of number and sizes of arbitrary particles using the disector. *J Microsc* 134: 127-136)
17. Woodman PG (2000) Biogenesis of the Sorting Endosome: The Role of Rab5. *Traffic* 1(9): 695–701
18. Weibel ER (1979) Stereological methods. Practical methods for biological morphometry. Vol. 1. Academic Press, London.